

# Structural and magneto-transport characterization of $\text{Co}_2\text{Cr}_x\text{Fe}_{1-x}\text{Al}$ Heusler alloy films

A. D. Rata, H. Braak, D. E. Bürgler,<sup>a</sup> S. Cramm, and C. M. Schneider

Institute of Solid State Research, Electronic Properties (IFF6) and

cni – Center of Nanoelectronic Systems for Information Technology, Research Center Jülich GmbH, D-52425 Jülich, Germany

Received: date / Revised version: date

**Abstract.** We investigate the structure and magneto-transport properties of thin films of the  $\text{Co}_2\text{Cr}_{0.6}\text{Fe}_{0.4}\text{Al}$  full-Heusler compound, which is predicted to be a half-metal by first-principles theoretical calculations. Thin films are deposited by magnetron sputtering at room temperature on various substrates in order to tune the growth from polycrystalline on thermally oxidized Si substrates to highly textured and even epitaxial on  $\text{MgO}(001)$  substrates, respectively. Our Heusler films are magnetically very soft and ferromagnetic with Curie temperatures up to 630 K. The total magnetic moment is reduced compared to the theoretical bulk value, but still comparable to values reported for films grown at elevated temperature. Polycrystalline Heusler films combined with MgO barriers are incorporated into magnetic tunnel junctions and yield 37% magnetoresistance at room temperature.

**PACS.** 75.47.-m Magnetotransport phenomena; materials for magnetotransport – 75.50.Cc Other ferromagnetic metals and alloys – 75.70.-i Magnetic properties of thin films, surfaces, and interfaces

## 1 Introduction

The efficient injection of spin currents into non-magnetic materials, which is a prerequisite for many future spintronic concepts [1] to work, requires materials with high

spin polarization of the conduction electrons [2]. Promising candidates are the so-called Heusler alloys [3]. So far, many Heusler compounds are predicted to show half-metallic properties from first-principles calculations [4, 5, 6]. They are characterized by a band gap at the Fermi energy only for one spin direction and metallic properties for the other. The charge carriers are thus 100% spin-

---

<sup>a</sup> *Corresponding author:* email d.buergler@fz-juelich.de, phone +49 2461 614214, FAX +49 2461 614443

polarized, rendering these materials ideal sources for efficient spin injection into semiconductors and for high magnetoresistance values in giant and tunneling magnetoresistance (GMR and TMR) devices. However, despite enormous experimental efforts, there has been no clear-cut experimental report yet on half-metallicity at room temperature (RT).

The Co-based full-Heusler compounds (*e.g.*,  $\text{Co}_2\text{Cr}_x\text{Fe}_{1-x}\text{Al}$ ,  $\text{Co}_2\text{MnSi}$ , and  $\text{Co}_2\text{MnGe}$ ) have been intensively investigated mainly because of their high Curie temperatures [7,8,9]. The specific  $L2_1$  structure of ordered full-Heusler alloys has the advantage of the absence of empty lattice sites compared to the half-Heusler compounds (*e.g.*,  $\text{NiMnSb}$ ) [10], which makes them less susceptible for site disorder. It is widely accepted now that structural disorder destroys the half-metallicity. In this respect,  $\text{NiMnSb}$  is a well studied example [11,12]. Site disorder is thus a critical factor for deteriorating the full spin polarization predicted for the perfectly ordered Heusler structure, particularly in very thin layers used in real devices. Yet, the question is to what extent site disorder is tolerable, *i.e.* leaves at least a high spin polarization value close to 100%. It has been predicted by Miura *et al.* [13] that in the case of the  $\text{Co}_2\text{CrAl}$  Heusler compound in the  $B2$  structural modification, site disorder between Cr and Al is less critical and allows for 84% spin polarization. Experimentally, Block *et al.* [14] have reported that  $\text{Co}_2\text{Cr}_{0.6}\text{Fe}_{0.4}\text{Al}$  (CCFA) bulk material in the ordered  $L2_1$  structure exhibits 30% magnetoresistance at RT in a magnetic field of 1 kOe. Shortly

thereafter, Inomata *et al.* [15] have found 16% TMR at RT in structures containing CCFA as one ferromagnetic electrode. These findings have motivated our work on the  $\text{Co}_2\text{CrAl}$  Heusler compound doped with Fe.

In this study, we investigate the structure and magnetic properties of CCFA thin films grown by magnetron sputtering. Various substrates (*e.g.*,  $\text{SiO}_2$ , GaAs, MgO) have been employed in order to tune the growth from polycrystalline on thermally oxidized Si substrates to highly textured and even epitaxial on MgO(001) substrates. Finally, we report on a high magnetoresistance value at RT in CCFA/MgO/CoFe junctions.

## 2 Experiment

$\text{Co}_2\text{Cr}_x\text{Fe}_{1-x}\text{Al}$  thin films with various thicknesses are grown by magnetron sputtering on  $\text{SiO}_2$  (thermally oxidized Si wafers), GaAs, and MgO substrates. The base pressure in our chamber is below  $1 \times 10^{-7}$  mbar and the sputtering Ar pressure is varied between  $1 \times 10^{-3}$  and  $3 \times 10^{-3}$  mbar. All substrates are cleaned *ex-situ* with solvents and immediately introduced into the vacuum chamber. The MgO substrates are further cleaned by annealing in vacuum at 392 K, whereas no *in-situ* treatment is done for  $\text{SiO}_2$  and GaAs substrates. We use stoichiometric  $\text{Co}_2\text{Cr}_x\text{Fe}_{1-x}\text{Al}$  targets with  $x = 0$  and  $x = 0.6$  for depositing our films. The sputtering rate, measured with a quartz balance, is set to 0.7 Å/s. The temperature of the substrate during the sputtering process is always RT. The influence of post-growth annealing treatments and the use of metal (*e.g.*, Cr, V) seed layers on the structural

and magnetic properties are also investigated. After deposition, the Heusler films can be annealed *in-situ* up to 873 K. The stoichiometry is checked *ex-situ* by secondary ions mass spectroscopy (SIMS). We find that the composition of our films is similar to the target compositions. The structure of the Heusler films is identified *ex-situ* by x-ray diffraction (XRD). Small-angle x-ray reflectivity (XRR) measurements are performed to determine the film thickness and to calibrate the sputtering rates. The XRD measurements are carried out with a Philips X'Pert MRD diffractometer using  $\text{Cu } K_\alpha$  radiation. Conductivity measurements are performed in the standard four-point geometry at temperatures between 10 and 300 K. For the magnetic characterization, we employed the magneto-optical Kerr effect (MOKE) and SQUID magnetometry. Some Heusler films are capped with a thin ( $\approx 30 \text{ \AA}$ ) Cu or  $\text{AlO}_x$  layer in order to investigate the interface properties by x-ray absorption spectroscopy (XAS) at the synchrotron.

### 3 Results

#### 3.1 Structural characterization

Figure 1 shows a wide  $\theta-2\theta$  XRD scan from a 100 nm-thick CCFA film grown at RT directly on a  $\text{SiO}_2$  substrate. Despite the low deposition temperature and the absence of any seed layer, which normally promotes textured growth, clear diffraction peaks are identified in the diffraction pattern. They indicate a polycrystalline morphology of the film. Ideally, for the characteristic  $L2_1$  structure of

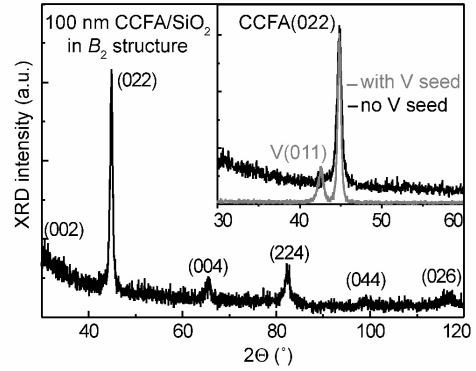


**Fig. 1.**  $\theta-2\theta$  XRD measurement of a 100 nm-thick CCFA film deposited on  $\text{SiO}_2$ . The inset compares part of the  $\theta-2\theta$  scan around the (022) Heusler peak from films deposited on  $\text{SiO}_2$  substrates with (grey) and without (black) a 40 nm-thick vanadium seed layer.

a Heusler compound, one should be able to distinguish in the XRD pattern besides the fundamental reflections, *e.g.* (022), two types of superlattice reflections, *i.e.* (111) and (002). Our CCFA films grown on amorphous, thermally oxidized Si wafers take the so-called  $B2$  (CsCl type) structure, where the absence of the (111) peak indicates complete disorder between Al and (Cr, Fe) atoms, while Co atoms occupy the correct sublattice. The same type of disordered structure has previously been observed in CCFA films by Inomata *et al.* [15]. When GaAs is used as a substrate (not shown), polycrystalline films with the same  $B2$  structure could only be obtained when a seed layer, *e.g.* Cr or V, is deposited prior the Heusler film. Otherwise we cannot observe any crystalline peaks in the XRD spectra, except for a broad (022) reflection on top of an amorphous background.

It has been shown by Geiersbach *et al.* [7] that, in order to grow highly textured Co-based Heusler thin films, vanadium is the best choice as a seed layer among Al, Cr, Cu, and V. In the inset of Fig. 1 we compare  $\theta-2\theta$  scans around the (022) diffraction peak from a 100 nm-thick CCFA film grown on  $\text{SiO}_2$  substrates with and without a 40 nm-thick vanadium seed layer, respectively. We also observe that the vanadium seed layer improves the texture of the Heusler films and that the amorphous-like background is completely suppressed. Further structural analysis is done by atomic force microscopy (AFM). In Fig. 2, we display two representative AFM pictures taken on the CCFA films discussed in the inset of Fig. 1. Quite surprising, the CCFA film grown directly on the  $\text{SiO}_2$  substrate is very smooth with a rms roughness of only 0.5 nm. A uniform distribution of grains with an average diameter of 40 nm is observed in Fig. 2(a). On the contrary, when vanadium is used as a seed layer, the grains' size is not as uniform and the roughness increases to  $\approx 1.0$  nm. The strain induced by the large lattice mismatch between

vanadium and the CCFA Heusler film might be an explanation for these observations.

Temperature is an important parameter in optimizing the structural and magnetic properties of Heusler compounds. Co-based alloy films, as for example  $\text{Co}_2\text{MnSi}$ ,  $\text{Co}_2\text{MnGe}$ , and  $\text{Co}_2\text{MnSn}$ , with ordered crystallographic structure could only be obtained by growing [7] or annealing [8] at relatively high temperatures above 700 K. Our CCFA films grow with good crystalline order already at RT. In order to study the influence of temperature on the structure and magnetic properties, we perform *in-situ* post-growth annealing experiments. The *in-situ* annealing treatment at temperatures up to 773 K has only little influence on the crystallographic structure of our films. We only observe a slight increase in the intensity of the diffraction peaks. On the other hand, changes in the magnetic properties are observed and will be discussed in Section 3.2.

It is well known that the choice of the substrate can drastically influence the structural characteristics and physical properties of a film. In order to improve the structure of the CCFA Heusler films we have chosen a single crystalline substrate, namely magnesium oxide. Kelekar and Clemens [16,17] prepared epitaxial CCFA films by magnetron sputtering onto a  $\text{MgO}(001)$  substrate held at 773 K. In Fig. 3 we present our XRD results of a 25 nm-thick CCFA film grown at RT on  $\text{MgO}(001)$  (black) in comparison with the data of the CCFA/ $\text{SiO}_2$  system from Fig. 1 (note the logarithmic scale in Fig. 3). The data clearly indicate epitaxial growth of CCFA films on

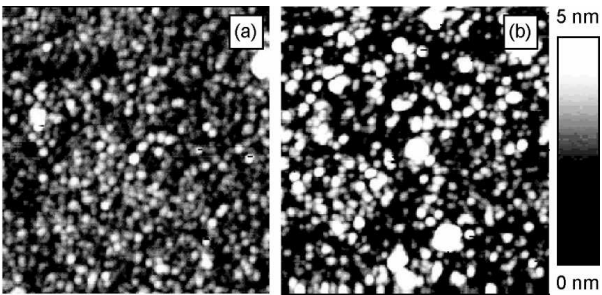


**Fig. 2.** Representative AFM pictures taken from 100 nm-thick CCFA films deposited on  $\text{SiO}_2$  without (a) and with (b) a vanadium seed layer. The size of the scans is  $1 \times 1 \mu\text{m}^2$ .

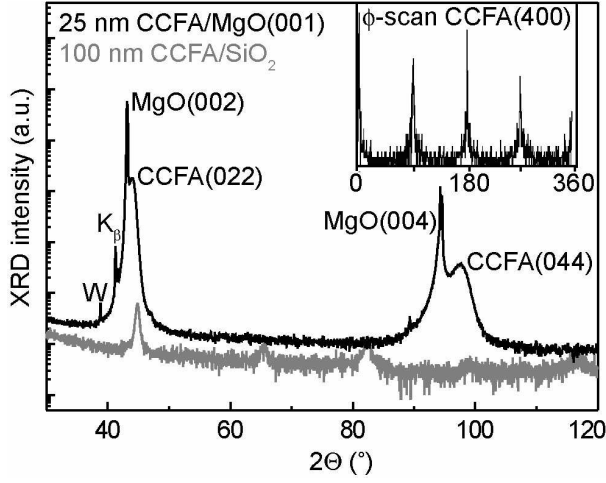


**Fig. 3.**  $\theta$ – $2\theta$  XRD measurement of a 25 nm-thick CCFA film deposited on MgO(001) (black) in comparison to the data of Fig. 1 (grey). Only the (022) and (044) diffraction peaks can be observed close to the (002) and (004) peaks characteristic of the MgO(001) substrate. MgO(002) Cu  $K_\beta$  and W  $L_\alpha$  peaks are indicated on the left of the (002) main MgO peak. Inset: In-plane  $\phi$ -scan through the (400) peaks of CCFA.

MgO(001) at RT. Only the (022) and (044) diffraction peaks of the film are observed close to (002) and (004) peaks of the MgO(001) substrate, indicating a highly oriented CCFA film on top of the rocksalt MgO substrate. The peaks originating from the film are broadened due to its finite thickness (25 nm). It is interesting to note that the [011] direction of the CCFA films is parallel to [001] of the MgO substrate. Thus, our films take a different orientation with respect to the MgO substrate compared to the results reported in Refs. [16,17], where  $\text{CCFA}[001]//\text{MgO}[001]$ . The lattice constant normal to the surface can be calculated from  $\theta$ – $2\theta$  scans by using Bragg’s law. We obtain a value of 5.81 Å, which is very close to the bulk value of 5.88 Å [14]. The lattice

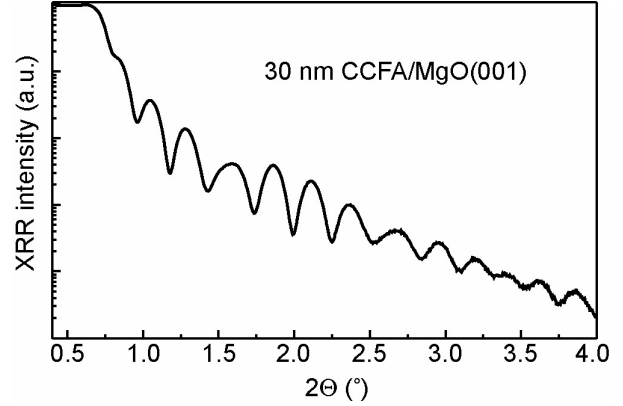


**Fig. 4.** Small angle XRR scan showing a well defined interface between the CCFA(011) film and the MgO(001) substrate.

constant of MgO is 4.21 Å, so the relatively small lattice mismatch (-1.3%) after a 45° in-plane rotation makes the MgO(001) surface a good template for epitaxial growth of CCFA films. For our epitaxial relationship, the unit cell of CCFA in the (011) plane at the interface is rectangular with an aspect ratio of  $\sqrt{2}$ . After the 45° rotation, the short edge points along either MgO[110] or MgO[-110] directions giving rise to two possible structural domains. Polar in-plane ( $\phi$ )-scans in the (011) plane of CCFA obtained by tilting the sample normal out of the scattering plane, reveal four-fold symmetry and, therefore, give definitive evidence for the epitaxial growth in two structural domains at RT. An example of a polar scan through the (400) Heusler peaks is shown in the inset of Fig. 3. Small angle XRR measurements show smooth and well defined interfaces between the Heusler film and the MgO substrate. A representative XRR spectrum is depicted in Fig. 4.

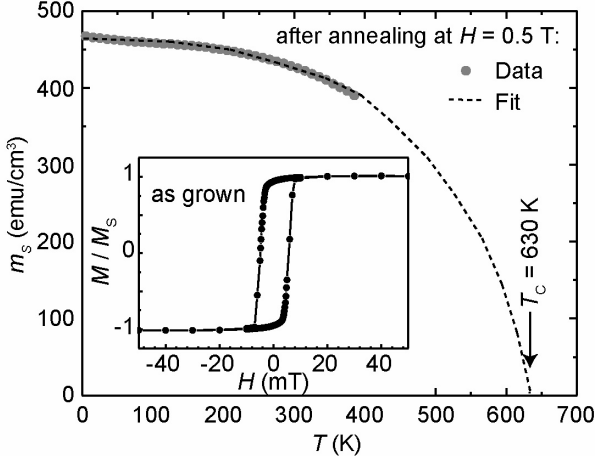


**Fig. 5.** Inset: Normalized magnetic hysteresis curve measured by SQUID at RT of an as-grown 100 nm-thick CCFA film on  $\text{SiO}_2$ . The main graph shows the temperature dependence of the saturation magnetization  $m_s$  of the same film after annealing in vacuum at 773 K for 1 hour together with the fitted Brillouin function. The Curie temperature is about 630 K.

### 3.2 Magnetic characterization

Our CCFA Heusler films display a soft ferromagnetic behavior. In the inset of Fig. 5 we present a normalized  $M$ - $H$  loop of a 100 nm-thick CCFA film grown on a  $\text{SiO}_2$  substrate. The coercive field is approximately 5 mT. Our films are magnetically softer compared to the recently reported results about CCFA films deposited on  $\text{Al}_2\text{O}_3$  substrates, which had a coercive field of 10 mT [18]. The Curie temperature of an as-grown film on a  $\text{SiO}_2$  substrate is estimated to be about 540 K from the extrapolation of the magnetization *versus* temperature curve (not shown). Annealing in vacuum at 773 K for one hour significantly increases the Curie temperature as shown by the temperature dependence of the saturation magnetization after

annealing in Fig. 5, where the solid line is a fitted Brillouin function yielding  $T_C \approx 630$  K.

The total magnetic moment obtained from the saturation magnetization at 5 K is 442  $\text{emu}/\text{cm}^3$  corresponding<sup>1</sup> to 2.42  $\mu_B$  per formula unit (f.u.) for as-grown films on  $\text{SiO}_2$ . After annealing in vacuum this value increases to 2.56  $\mu_B/\text{f.u.}$  (467  $\text{emu}/\text{cm}^3$ ). Magnetic moments, Curie temperatures, and coercive fields for CCFA films grown on various substrate systems are compiled in Table 1. The lower Curie temperatures for the film grown on MgO might be related to the reduced thickness. The magnetic properties do not strongly vary for different substrates, in spite of the quite different film structures. But in all cases the post-annealing increases the magnetic moment as well as the Curie temperature, which both are governed by the film volume. All films are relatively soft with  $H_C$

<sup>1</sup> The volume per f.u. is  $(5.88 \text{ \AA})^3/4$  and  $1 \text{ emu} = 1.079 \times 10^{20} \mu_B$ .

**Table 1.** Magnetic moment  $m_s$  at 5 K, Curie temperature  $T_C$ , and coercive field  $H_C$  of CCFA films grown on different substrates in the as-grown and 773 K post-annealed state.

Substrate	thickness (nm)	state	$m_s$ ( $\mu_B/\text{f.u.}$ )	$T_C$ (K)	$H_C$ (mT)
$\text{SiO}_2$	100	as-grown	2.42	540	5
	100	annealed	2.56	630	5-6
40 nm V	100	as-grown	2.43	575	7
	100	annealed	2.52	590	7
MgO	25	as-grown	2.46	380	6
	25	annealed	2.56	500	6

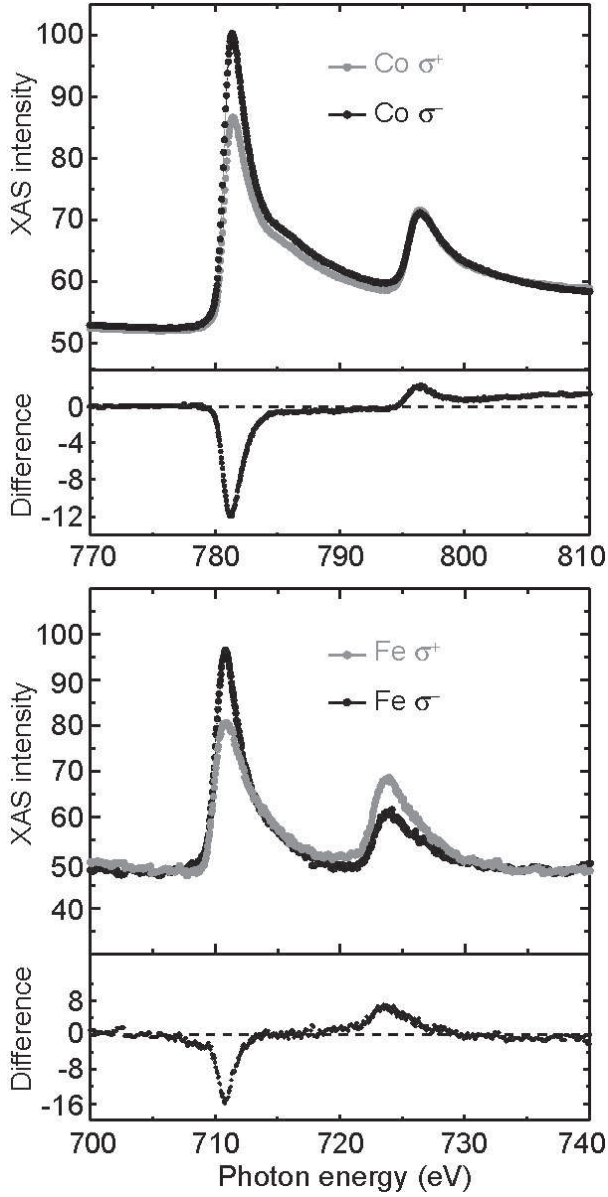


**Fig. 6.** XMCD-XAS spectra at the Co and Fe  $L_{23}$  edges show clear magnetic signals and indicate parallel alignment of the Co and Fe moments.

in the range from 5 to 7 mT. These findings are in agreement with results from FMR measurements of our CCFA samples performed by Rameev *et al.* [19].

The measured magnetic moments per formula unit are small compared to the theoretical value for ordered CCFA with  $L_{21}$  structure, which is  $3.8 \mu_B/\text{f.u.}$  [6]. On the other

hand, our values are comparable to the data reported for films grown at elevated temperatures [16,17]. These authors also found a reduced experimental magnetic moment as compared to the calculated moment for Cr-containing samples. Only the magnetic moment of  $\text{Co}_2\text{FeAl}$  reaches the predicted value of  $4.9 \mu_B/\text{f.u.}$  [20]. Moreover, even the magnetic moment measured in bulk samples is smaller than the calculated one [21,22]. It is generally recognized that the magnetic moments and the degree of spin polarization are critically dependent on the chemical disorder [23]. Despite the fact that our CCFA Heusler films have a rather good crystallographic order, site disorder seems to play a critical role for the Curie temperature and the total magnetic moment. It is not possible to determine the site disorder in CCFA films from XRD, because Co, Cr, and Fe have very similar scattering factors. Neutron scattering experiments could give more insight about the degree of chemical disorder in the Heusler films.

We gain additional information on the presence of site disorder in our films from XAS by measuring the x-ray magnetic circular dichroism (XMCD). CCFA films, covered with a thin  $\text{AlO}_x$  cap layer are investigated exciting with circular polarized light at the Co, Fe, and Cr  $L_{23}$  edges. The measurements are done in the total-yield mode, where one directly measures the sample current while scanning the photon energy. The finite escape depth of the photoelectrons limits the information depth to the interface region. The sample current is normalized to the photon intensity measured on a gold mesh. The magnetic field applied to the sample (0.25 T) is aligned with the

surface normal and lies at an angle of about  $30^\circ$  with respect to the incident photon direction. The line shape of the XAS spectra is that of metallic (*e.g.* non-oxidized) Co and Fe. We obtain a clear dichroic signal at both the Co and Fe edges, which indicates for the interface region ordered Co and Fe spins with parallel alignment (see Fig. 6). In contrast, no magnetic dichroism is observed at the Cr edge (not shown). This is an indication for partially antiparallel alignment of the Cr interfacial spins with respect to each other, which can be related to the presence of site disorder. This result could also explain the reduced values of the Curie temperature and the magnetic moment compared to the bulk material. Moreover, we find that a selective oxidation of Cr always occurs for CCFA capped with 3 nm of Cu, while 3 nm-thick  $\text{AlO}_x$  layers protect the CCFA films against oxidation. A quantitative analysis of XAS-XMCD measurements performed on CCFA Heusler compounds has been reported by Elmers *et al.* [21,22].

### 3.3 Transport properties

Resistivity measurements with the current flowing in the plane of the sample reveal a metallic behavior, with the resistivity increasing with increasing temperature as shown in Fig. 7 for a 50 nm-thick CCFA film covered with 3 nm of  $\text{AlO}_x$ . The residual resistivity at 10 K is quite low,  $\approx 10^{-5} \Omega\text{cm}$ , and the temperature dependence is rather weak. This anomalous behavior of the temperature-dependent resistivity has also been observed in Ni-based Heusler compounds, and it was interpreted as a characteristics of disordered metallic systems [24].

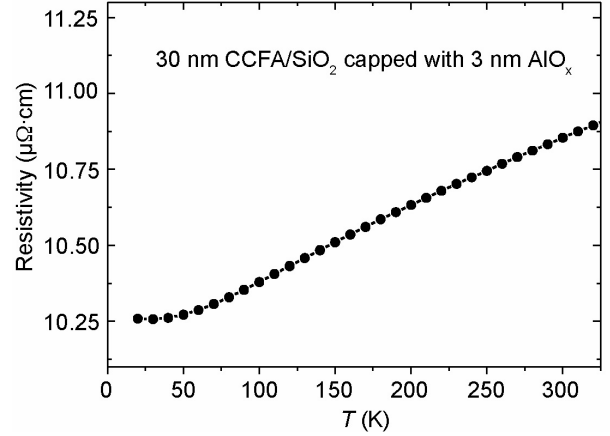


**Fig. 7.** In-plane resistivity of a 50 nm-thick CCFA film covered with a 3 nm-thick  $\text{AlO}_x$  cap layer indicating metallic conductivity down to 10 K.

Recently, relatively high TMR ratios have been obtained using Co-based full-Heusler alloy thin films, *i.e.*  $\text{Co}_2\text{MnSi}$  [25],  $\text{Co}_2\text{FeAl}$  [26], and CCFA [15,27,28]. Owing to the good structural quality and the well oriented growth of our CCFA films on MgO, we have integrated them into TMR structures with MgO as tunneling barrier. MgO has recently been proven to be a well behaved barrier material yielding very high TMR ratios in fully epitaxial Fe/MgO/Fe [29] and sputtered CoFe/MgO/CoFe structures with highly oriented MgO barriers [30].

The layered TMR structures are prepared by magnetron sputtering without breaking the vacuum with the following layer sequence:  $\text{SiO}_2/\text{CCFA}(25 \text{ nm})/\text{MgO}(3 \text{ nm})/\text{CoFe}(5 \text{ nm})/\text{IrMn}(15 \text{ nm})$ . In some cases a 40 nm-thick MgO layer is deposited on the substrate to improve the texture of the CCFA electrode. All layers in the structure are successively sputtered at RT. The MgO barrier is deposited by rf-stimulated discharge from a stoichiometric target. The sputtering



rate is calibrated by measuring the thickness of a MgO film by XRR. Here we present results for magnetic tunnel junctions containing CCFA as bottom ferromagnetic electrode, deposited directly on a  $\text{SiO}_2$  substrate. The completed stack is annealed *in-situ* for 1 hour at 523 K. Although an IrMn antiferromagnet is employed to pin the magnetization of the upper CoFe electrode, the two ferromagnetic layers do not switch separately, as observed in SQUID measurements. We mention at this point that no magnetic field can be applied during the *in-situ* annealing. Thus, no magnetic alignment by field cooling is introduced to this structure to induce an exchange bias. Junctions with an area from  $3 \times 3$  up to  $15 \times 15 \mu\text{m}^2$  with crossed electrodes are patterned for magnetotransport measurements in the current-perpendicular-plane (CPP) geometry by standard optical lithography.

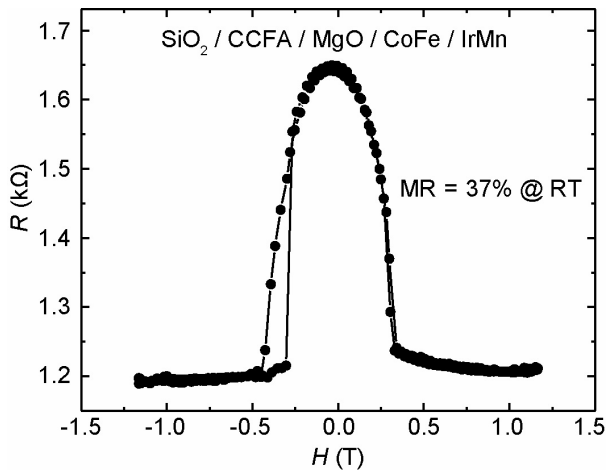


**Fig. 8.** Magnetoresistance curve of a  $10 \times 10 \mu\text{m}^2$  junction with layer sequence  $\text{SiO}_2/\text{CCFA}(25 \text{ nm})/\text{MgO}(3 \text{ nm})/\text{CoFe}(5 \text{ nm})/\text{IrMn}(15 \text{ nm})$ . The measurement is performed at RT and yields a magnetoresistance of 37%.

In Fig. 8 we show the magnetoresistance curve measured at RT. The TMR ratio defined as  $\text{TMR} = (R_{AP} - R_P)/R_P$ , where  $R_{AP}$  and  $R_P$  are the resistances for the antiparallel and parallel magnetization configurations, respectively, reaches 37%. The resistance-area product is about  $100 \text{ k}\Omega\mu\text{m}^2$ . This is a relatively large value for structures comprising a ferromagnetic Heusler electrode. Further investigations of the magnetotransport properties of TMR structures grown with the optimized parameters reported in this work are in progress and will be detailed in an upcoming report [31].

## 4 Summary

To summarize, we succeeded in preparing high quality  $\text{Co}_2\text{Cr}_{0.6}\text{Fe}_{0.4}\text{Al}$  (CCFA) Heusler alloy thin films using magnetron sputtering at RT. Various substrates ( $\text{SiO}_2$ , GaAs, MgO) were employed in order to tune the growth from polycrystalline on thermally oxidized Si substrates to highly textured and even epitaxial on  $\text{MgO}(001)$  substrates. We studied the influence of post-growth *in-situ* annealing treatments and the use of Cr and in particular V seed layers on the structural and magnetic properties. Magnetization measurements revealed ferromagnetic ordering. The Curie temperatures could be increased up to 630 K after annealing in vacuum at 773 K. XRD measurements indicated a high quality of the films grown on MgO substrates with well defined interfaces and low roughness, while the films grow in a polycrystalline fashion on  $\text{SiO}_2$ . Although our films grow at RT in a different orientation on the  $\text{MgO}(001)$  substrate than reported in Refs. [16,17],

the total magnetic moments are very similar with values of about  $2.5 \mu_B/\text{f.u.}$ . Therefore, the structural order is less important for the size of the magnetic moment. This is also reflected by the rather constant value of the magnetic moment for the various substrates, which give rise to quite different structural properties. In accordance with the theoretical result of Picozzi *et al.* [23] we conclude that the site disorder is the relevant parameter which determines the size of the magnetic moment and the Curie temperature in thin films.

Finally, we observed large magnetoresistance values of up to  $\approx 40\%$  at RT in TMR structures containing a polycrystalline CCFA film directly grown on  $\text{SiO}_2$  as a bottom ferromagnetic electrode and MgO as a tunneling barrier, both deposited by magnetron sputtering at RT. These preliminary transport measurements are encouraging for further investigations of TMR structures consisting of highly-oriented or epitaxial Co-based full-Heusler alloy films combined with possibly epitaxial MgO tunneling barriers. We expect a strong dependence on the film structure (*i.e.* choice of the substrate), much higher TMR ratios, and insight into the half-metallic properties of Heusler alloys at the interface, because the tunneling effect is very sensitive to the interface properties.

We would like to thank F.-J. Köhne for technical support, P. Erhart for the possibility of using the x-ray diffractometer, H. Elmers, M. Ležaić, and P. Grünberg for discussions and useful suggestions.

## References

1. S. A. Wolf, D. D. Awschalom, R. A. Buhrman, J. M. Daughton, S. von Molnár, M. L. Roukes, A. Y. Chtchelkanova, and D. M. Treger, *Science* **294**, 1488 (2001).
2. G. Schmidt, D. Ferrand, L. W. Molenkamp, A. T. Filip, and B. J. van Wees, *Phys. Rev. B* **62**, R4790 (2000).
3. F. Heusler, *Verh. Dtsch. Phys. Ges.* **5**, 219 (1903).
4. R. A. de Groot, F. M. Mueller, P. G. van Engen, and K. H. J. Buschow, *Phys. Rev. Lett.* **50**, 2024 (1983).
5. I. Galanakis, P. H. Dederichs, and N. Papanikolaou, *Phys. Rev. B* **66**, 134428 (2002).
6. I. Galanakis, P. H. Dederichs, and N. Papanikolaou, *Phys. Rev. B* **66**, 174429 (2002).
7. U. Geiersbach, A. Bergmann, and K. Westerholt, *J. Magn. Mater.* **240**, 546 (2002).
8. J. Schmalhorst, S. Kämmerer, M. Sacher, G. Reiss, A. Hütten, and A. Scholl, *Phys. Rev. B* **70**, 024426 (2004).
9. W. H. Wang, M. Przybylski, W. Kuch, L. I. Chelaru, J. Wang, Y. F. Lu, J. Barthel, H. L. Meyerheim, and J. Kirschner, *Phys. Rev. B* **71**, 144416 (2005).
10. *Magnetic properties of metals*, edited by H. P. J. Wijn (Springer, Berlin, 1991).
11. K. E. H. M. Hanssen and P. E. Mijnen, *Phys. Rev. B* **34**, 5009 (1986).
12. D. Ristoiu, J. P. Nozières, C. N. Borca, T. Komesu, H.-K. Jeong, and P. A. Dowben, *Europhys. Lett.* **49**, 624 (2000).
13. Y. Miura, K. Nagao, and M. Shirai, *Phys. Rev. B* **69**, 144413 (2004).
14. T. Block, C. Felser, G. Jakob, and J. Ensling, *J. Solid State Chem.* **176**, 646 (2003).
15. K. Inomata, S. Okamura, R. Goto, and N. Tezuka, *Jpn. J. Appl. Phys.* **42**, L419, (2003).

16. R. Kelekar and B. M. Clemens, *J. Appl. Phys.* **96**, 540 (2004).
17. R. Kelekar and B. M. Clemens, *Appl. Phys. Lett.* **86**, 232501 (2005).
18. G. Jakob, F. Casper, V. Beaumont, S. Falk, N. Auth, H. J. Elmers, C. Felser, and H. Adrian, *J. Magn. Magn. Mater.* **290**, 1104 (2005).
19. B. Rameev, F. Yildiz, S. Kazan, B. Aktas, A. Gupta, L. Tagirov, D. Rata, D. E. Bürgler, P. Grünberg, C. M. Schneider, S. Kämmerer, G. Reiss, and A. Hütten, *phys. stat. sol.*, in press (2006).
20. I. Galanakis, *J. Phys.: Condens. Matter* **16**, 3089 (2004).
21. H. J. Elmers, G. H. Fecher, D. Valdaitsev, S. A. Nepijko, A. Gloskovskii, G. Jakob, G. Schönhense, S. Wurmehl, T. Block, C. Felser, P.-C. Hsu, W.-L. Tsai, and S. Cramm, *Phys. Rev. B* **67**, 104412 (2003).
22. H. J. Elmers, S. Wurmehl, G.H. Fecher, and G. Jakob, *Appl. Phys. A* **79**, 557 (2004).
23. S. Picozzi, A. Contineza, and A. J. Freeman, *Phys. Rev. B* **69**, 094423 (2004).
24. K. Ahilan, M. C. Bennett, M. C. Aronson, N. E. Anderson, P. C. Canfield, E. Munoz-Sandoval, T. Gortenmulder, R. Hendrikx, and J. A. Mydosh, *Phys. Rev. B* **69**, 245116 (2004).
25. J. Schmalhorst, S. Kämmerer, G. Reiss, and A. Hütten, *Appl. Phys. Lett.* **86**, 052501 (2005).
26. S. Okamura, A. Miyazaki, S. Sugimoto, N. Tezuka, and K. Inomata, *Appl. Phys. Lett.* **86**, 232503 (2005).
27. K. Inomata, S. Okamura, and N. Tezuka, *J. Magn. Magn. Mater.* **282**, 269 (2004).
28. T. Marukame, T. Kasahara, K. Matsuda, T. Uemura, and M. Yamamoto, *Jap. J. Appl. Phys.* **44**, L521 (2005).
29. S. Yuasa, T. Nagahama, A. Fukushima, Y. Suzuki, and K. Ando, *Nature Materials* **3**, 868 (2004).
30. S. S. P. Parkin, C. Kaiser, A. Panchula, P. M. Rice, B. Hughes, M. Samant, and S.-H. Yang, *Nature Materials* **3**, 862 (2004).
31. A. D. Rata, H. Braak, D. E. Bürgler, and C. M. Schneider, unpublished.